Supporting Information

Controllable architecture of the NiCoZnS@NiCoFe layered double hydroxide coral-like structure for high-performance supercapacitors

Shi-Bing Lv, Hong-Yan Zeng*, Kai-Min Zou, Shen Xu, Yi-Wen Long, Hao-Bo Li, Zhen Li

College of Chemical Engineering, Xiangtan University, Xiangtan 411105, Hunan, China

*Corresponding Author

Hong-Yan Zeng

E-mail address: hongyanzeng99@hotmail.com; hyzeng@xtu.edu.cn

Fig. S1 EDX pattern of the NiCoFe-LDH with the Ni/Co/Fe molar ratio of 1: 1: 1.

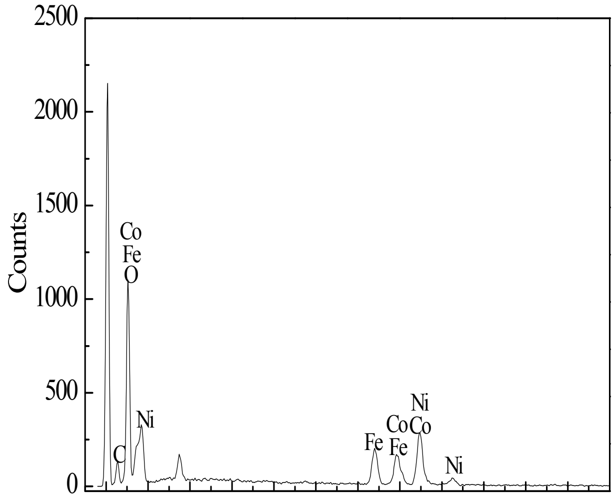

The semi-quantitative EDS was used to detect the chemical constitution, which showed that Ni, Co, Fe, C and O elements were present in the NiCoFe-LDH sample.

Fig. S2 CV curves (A), plots (B) of anodic and cathodic peak currents vs. square root of scan rate, GCD curves (C), corresponding C_S (D) at various current densities, Nyquist plot (E) and cyclic stability (F) for the NiCoFe-LDH on NF.

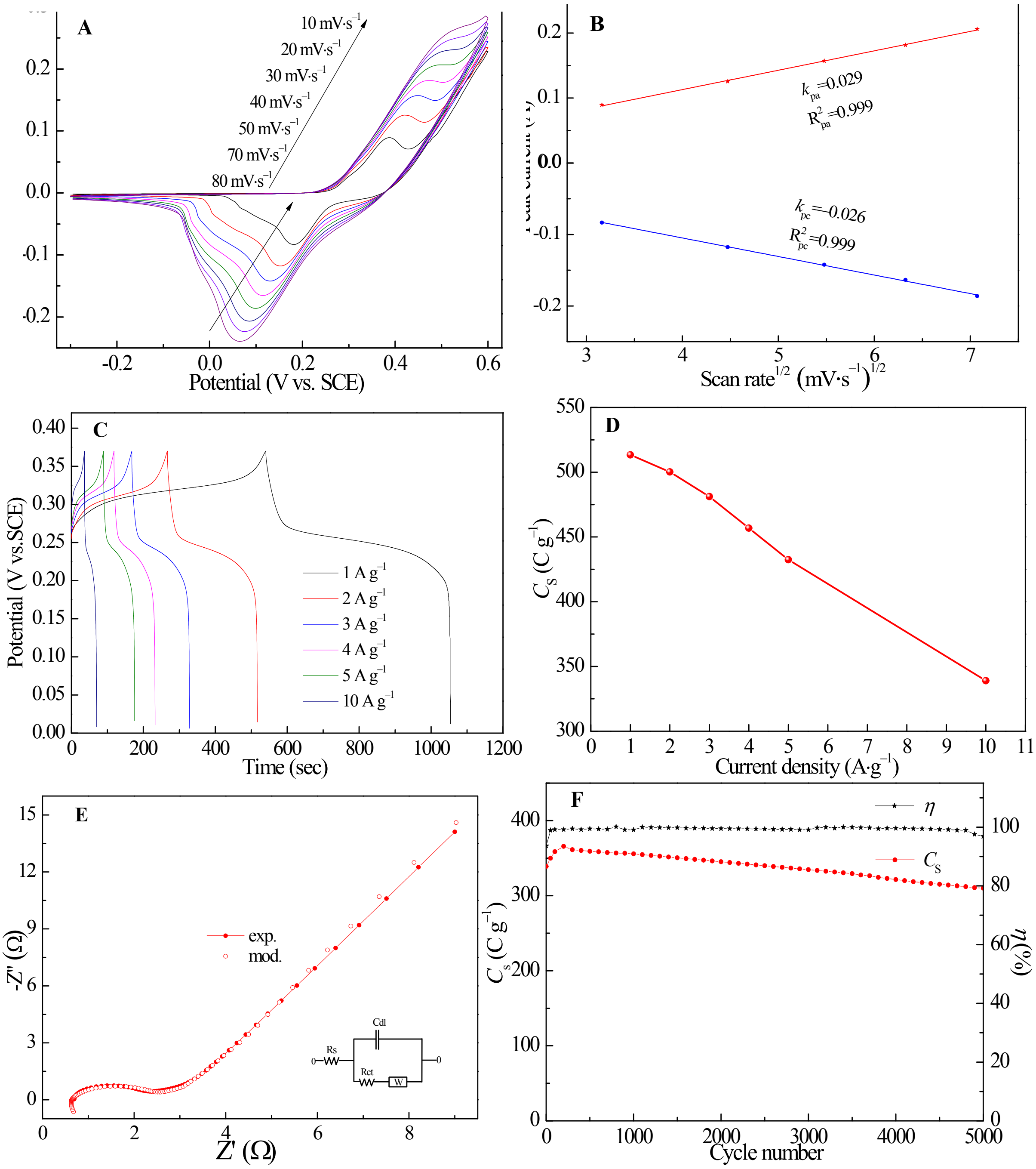

The cyclic voltammograms (CV), electrochemical impedance spectroscopy (EIS) and galvanostatic charge-discharge (GCD) were conducted on a CHI660D electrochemical workstation (Shanghai Chenhua Apparatus Co. Ltd., Shanghai, China), which were performed in 6.0 mol·L^{-1} KOH solution using a three electrode system. The NiCoFe-LDH on NF (1×1 cm^2

in quadrate shape) as the working electrode, while the saturated calomel electrode (SCE) and platinum foil were used as reference and counter electrodes, respectively. CV were determined in the potential range between −0.3 and 0.6 V (vs. SCE) for the 12th cycle, while the GCD were gained between 0 and 0.37 V (vs. SCE) for the first cycle. EIS was performed between 0.01 Hz to 100 KHz under open circuit voltage conditions with perturbation voltage at 5 mV. The cycle stability was evaluated at 10 A g^{-1} for 5 000 cycles, in which the last 20 constant GCD curves (Fig. S2f inset) were obtained. The NiCoFe-LDH electrode exhibited a pair of redox peaks due to the Faradaic redox process. The shape of the CV curves at different scan rates had hardly a change along with the change of scan rate, revealing the high specific capacitance and good reversibility (Fig. S2a). The anodic and cathodic peak currents were linearly related to the square root of scan rate ($R^2 = 0.999$), suggesting the diffusion-controlled process (Fig. S2b). As seen in Fig. S2c, the *C*s values at 1.0, 2.0, 3.0, 4.0, 5.0 and 10.0 A g^{-1} were 513.4 C g^{-1} (1387.6 F·g^{-1}), 500.2 C g^{-1} (1351.9 F g^{-1}), 481.2 C g^{-1} (1300.5 F g^{-1}), 456.8 C·g^{-1}(1234.6 F g^{-1}), 432.5 C g^{-1} (1169 F g^{-1}), and 339.0 C g^{-1} (916.2 F g^{-1}), respectively. The *C*s decreased gradually with increasing the current density, in which the *C*s value was still maintained about 66.03% of the *C*s value at 1.0 A g^{-1} even at a high discharge current density of 10.0 A g^{-1} (Fig. S2d). Furthermore, the interfacial charge transfer resistance (R_{ct}) and intrinsic resistance (R_s) were obtained by fitting the EIS data to a suitable equivalent circuit from models using Zview2.0 software (Chi square value 6.90×10^{-3}) in Fig. S2e, where the R_{ct} and R_s values were 0.686 and 1.310 Ω, respectively. At the same time, the NiCoFe-LDH electrode exhibited a cycle stability of 91.44% of its initial *C*s (339.0 C g^{-1}, or 916.2 F g^{-1}) and 96.88% of its the Coulomb efficiency (η) at 10 A g^{-1} for 5 000 cycles, suggesting that the NiCoFe-LDH was a good electrode material for supercapacitors.

Fig. S3 SEM images of the NF(A) and NiCoFe-LDH (B,C).

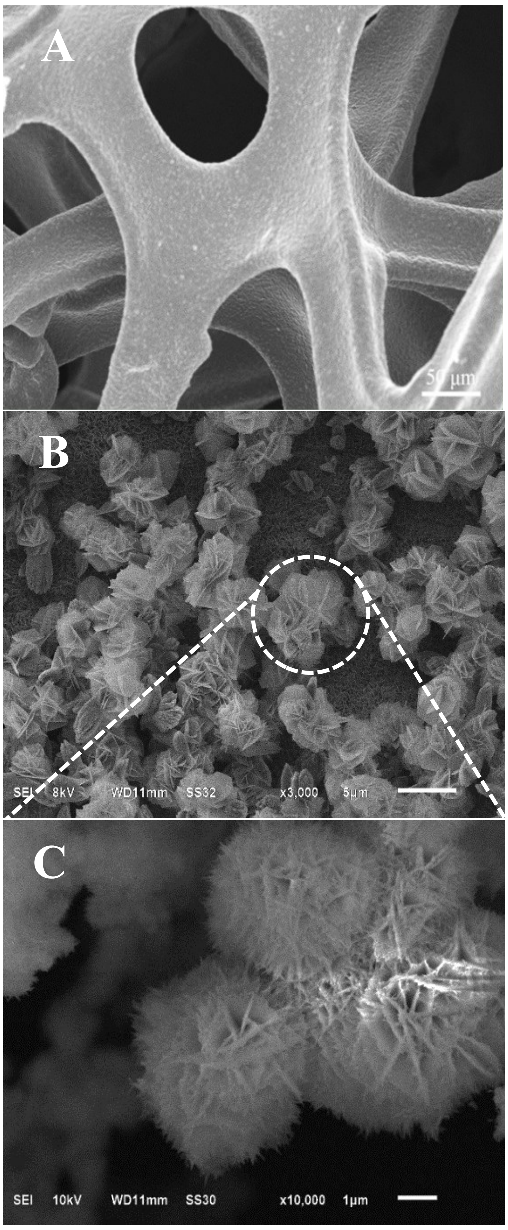

Fig. S4 FT-IR spectra of the NiCoFe-LDH, $NiCoZnS_1$ and NiCoZnS@NiCoFe-LDH.

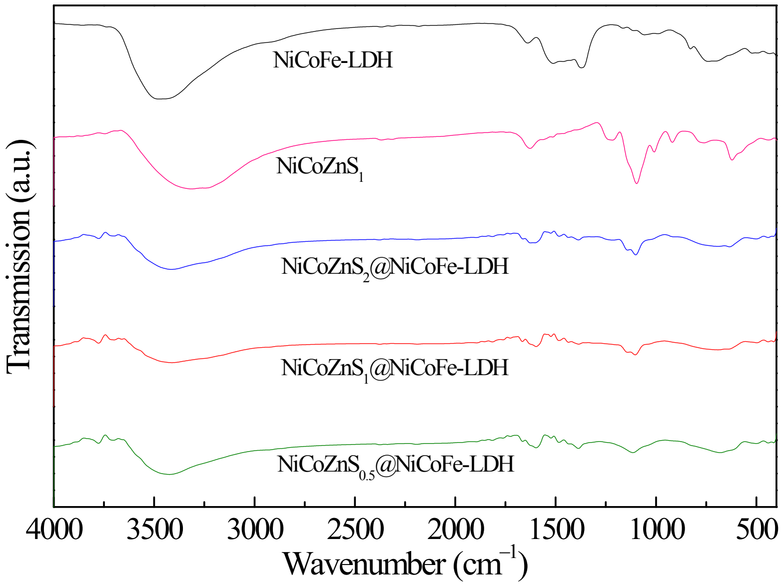

The FT-IR spectra of the samples in the region 400~4000 cm^{-1} are shown in Fig. S4, in which the spectra of the $NiCoZnS_1$ and NiCoZnS@NiCoFe-LDH samples were basically similar. As seen in Fig. S4, the FT-IR spectra of the NiCoFe-LDH was the same as that of a typical hydrotalcite, in which the peaks at around 3482 cm^{-1} (structural–OH group), 1376 cm^{-1} (CO_3^{2-} group in the interlayers) and 1650 cm^{-1} (H_2O molecule) were detected. The peaks below 1000 cm^{-1} were assigned to metal-oxygen bond (M-O, M-O-M and M-OH, M: Ni^{2+}, Co^{2+} and Fe^{3+}) skeletal vibrations [1]. For the Ni_1Co_1ZnS, the peaks at about 1621 cm^{-1} (H_2O molecule) and 1091 cm^{-1} (Co=S) were observed, indicating the presence of cobalt sulfide [1]. Furthermore, the FT-IR spectrum of the NiCoZnS@NiCoFe-LDH was generally similar to that of the $NiCoZnS_1$ except for a minor difference, in which a new peak at about 1376 cm^{-1} appeared due to the interlayer-CO_3^{2-} from the NiCoFe-LDH loaded on the surface of the NiCoZnS. Furthermore, the peak at around 3482 cm^{-1} (structural–OH group) shifted to high wavenumber owing to the combination of the NiCoFe-LDH with NiCoZnS cores.

References

1. Y. W. Long, H. Y. Zeng, H. B. Li, K. M. Zou, S. Xu and X. J. Cao, *Electrochim. Acta* 2020, 361, 137098

Fig. S5 CV curves of the NiCoZnS$_2$@NiCoFe-LDH (A), NiCoZnS$_{0.5}$@NiCoFe-LDH (B) and NiCoZnS$_1$ (C).

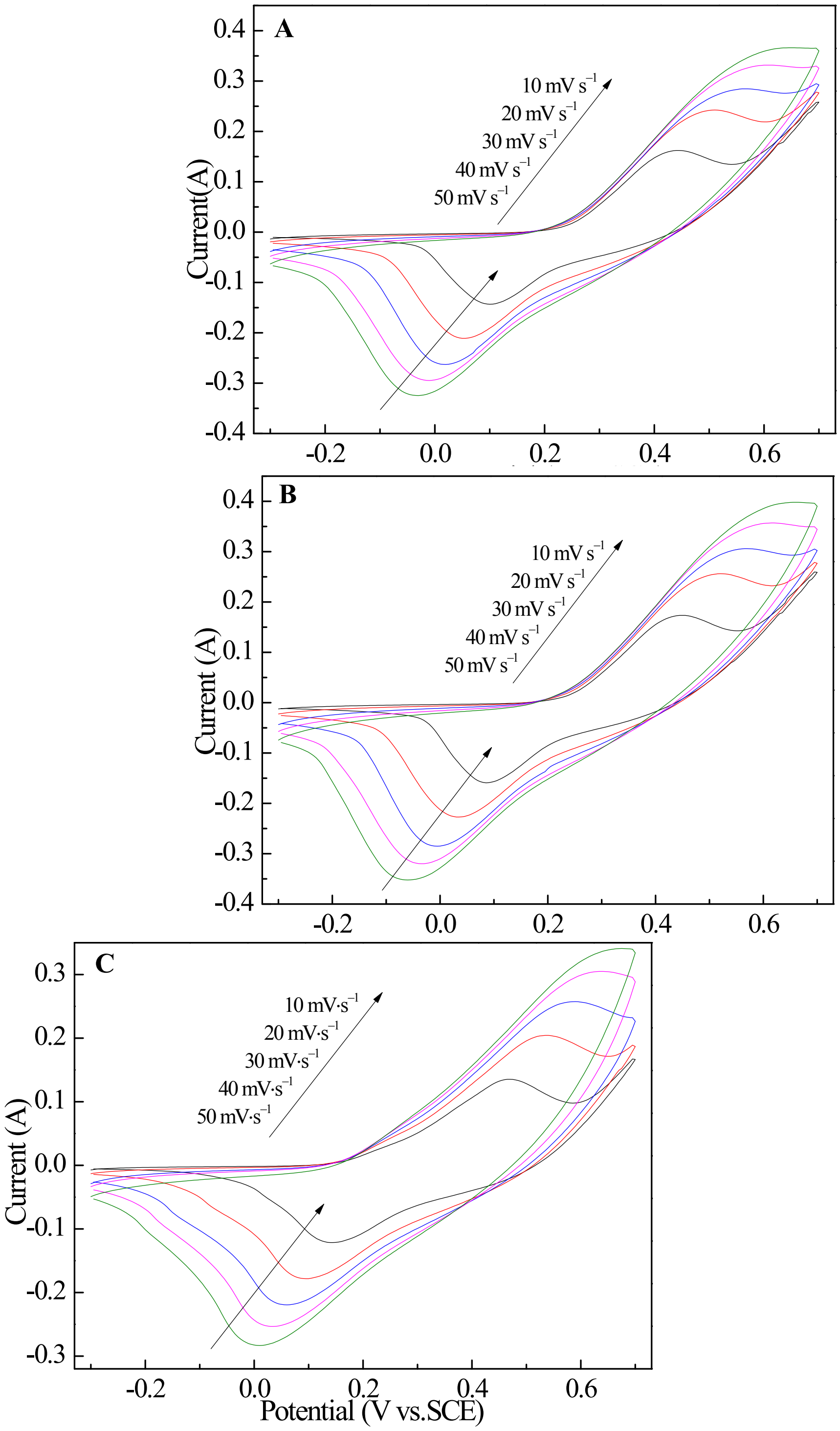

Fig. S6 GCD curves of the NiCoZnS$_2$@NiCoFe-LDH(A) and NiCoZnS$_{0.5}$@NiCoFe-LDH(B).

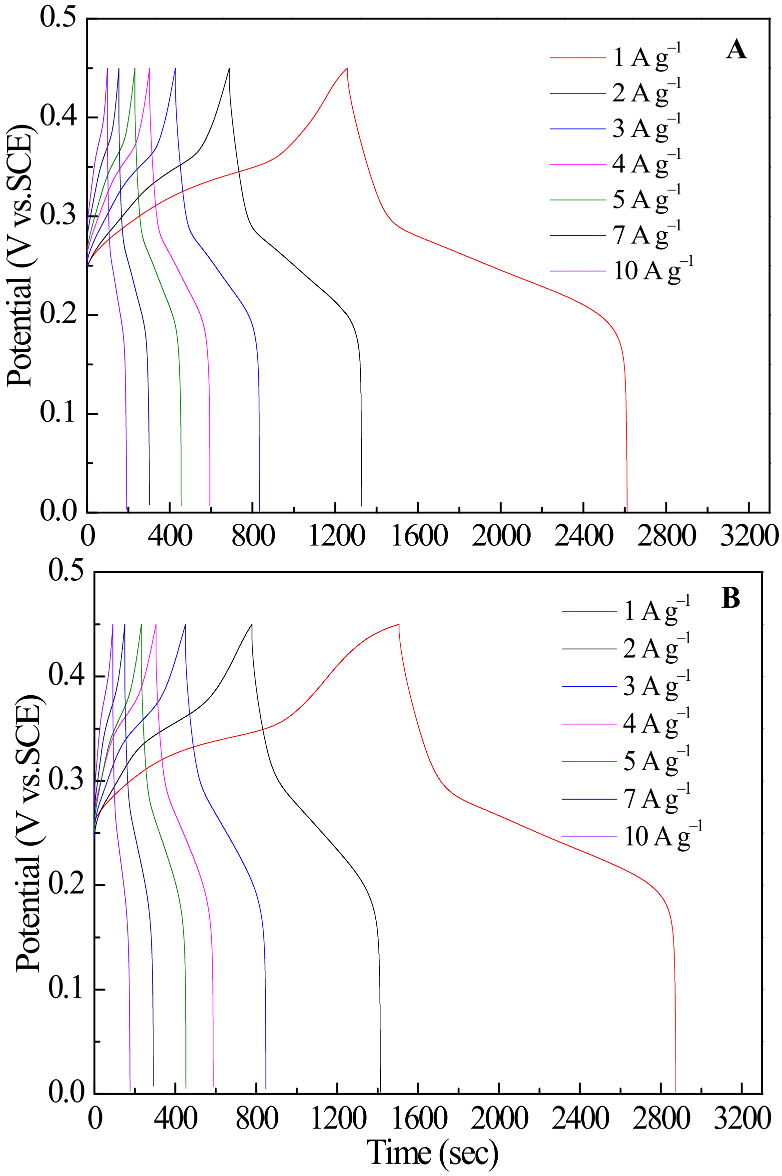

Table S1 CV behavior for the as-prepared samples

	b (R^2)	Anodic peak		Cathodic peak	
		k_{pa}	r^2	k_{pc}	r^2
NiCoFe-LDH	0.521 (0.999)	0.029	0.999	-0.026	0.999
$NiCoZnS_1$	0.577 (0.999)	0.053	0.999	-0.041	0.999
$NiCoZnS_2$@NiCoFe-LDH	0.478 (0.989)	0.046	0.956	-0.047	0.993
$NiCoZnS_1$@NiCoFe-LDH	0.506 (0.999)	0.060	0.998	-0.053	0.995
$NiCoZnS_{0.5}$@NiCoFe-LDH	0.512 (0.997)	0.057	0.998	-0.050	0.995